DOI: 10.1002/cphc.201000854

Incorporating Multiple Energy Relay Dyes in Liquid Dye-Sensitized Solar Cells

Jun-Ho Yum,[a] Brian E. Hardin,[b] Eric T. Hoke,[c] Etienne Baranoff,[a] Shaik M. Zakeeruddin,[a] Mohammad K. Nazeeruddin,[a] Tomas Torres,[d, e] Michael D. McGehee,[b] and Michael Grätzel*[a]

Panchromatic response is essential to increase the light-harvesting efficiency in solar conversion systems. Herein we show increased light harvesting from using multiple energy relay dyes inside dye-sensitized solar cells. Additional photoresponse from 400–590 nm matching the optical window of the zinc phthalocyanine sensitizer was observed due to Förster resonance energy transfer (FRET) from the two energy relay dyes to the sensitizing dye. The complementary absorption spectra of the energy relay dyes and high excitation transfer efficiencies result in a 35% increase in photovoltaic performance.

1. Introduction

The dye-sensitized mesoscopic solar cell (DSC) has been intensively investigated as a promising photovoltaic cell. Its ecological and economical fabrication processes make it an attractive alternative to conventional photovoltaic systems.[1] Panchromatic response is essential to increase the light-harvesting efficiency in solar cells.[2] In this respect, long-range energy transfer has recently been used to increase light harvesting inside the DSCs.[3–7] In our architecture, energy relay dyes (ERDs) absorb high-energy photons and transfer energy via Förster resonance energy transfer (FRET) to the sensitizing dyes. FRET involves dipole–dipole coupling of two chromophores, known as the donor and acceptor, through an electric field.[8] ERDs have a fundamentally different function and design rules from sensitizing dyes and thus this architecture greatly expands the range of dyes for DSC application. In order for ERDs to be used in state-of-the-art dye-sensitized solar cells, they must be able to strongly absorb the higher energy portion of the solar spectrum and efficiently transfer energy to the sensitizing dyes. Recently, we have reported excitation transfer efficiencies (ETEs) of over 95% by incorporating the commercially available laser dye, 4-(dicyanomethylene)-2-methyl-6-(4-dimethylaminostyryl)-4*H*-pyran (DCM),[9] with zinc phthalocyanine, TT1.[10,11] TT1 exhibits a high molar absorption coefficient around 700 nm with an optical window between 400–590 nm. The incorporated DCM harvests solar photons between 400–550 nm. It was shown that due to FRET from DCM to TT1, the photocurrent density is increased, augmenting the power conversion efficiency (PCE) of the DSC by $>25\%$.[11]

One strong advantage of the ERD concept over cosensitization, where all dyes attach at the TiO_2 surface,[12–13] is the ability to easily include multiple dyes with complementary absorption spectra. In cosensitization, the limited number of sites on the TiO_2 surface to which dye molecules attach places a constraint on the light absorption. In the ERD architecture, placing multiple energy relay dyes inside the electrolyte would allow for greater light harvesting. Hence, large concentrations of energy relay dyes can be placed inside of the electrolyte to absorb light in the visible spectrum and relay energy through long-range FRET to the dye attached at the surface. It is also possible to place multiple ERDs with complementary absorption spectra to maximize light absorption inside the device.

Herein we employ two commercially available dyes, DCM[9] and Rhodamine B (RB)[14] with complementary absorption spectra, resulting in high yields of excitation transfer when placed inside the porous network of the nanocrystalline TiO_2 film of a DSC. This increases the solar-to-electric power conversion efficiency (PCE) by 35%. These devices perform significantly better than devices where only one of the energy relay dyes is used. The increased light harvesting is primarily attributed to FRET from both relay dyes directly to the TT1 sensitizing dye.

[a] *Dr. J.-H. Yum,[+] Dr. E. Baranoff, Dr. S. M. Zakeeruddin, Dr. M. K. Nazeeruddin, Prof. M. Grätzel*
Institute of Chemical Sciences and Engineering
Ecole Polytechnique Fédérale de Lausanne
CH-1015 Lausanne, Switzerland
Fax: (+41) 21-693-4111
E-mail: michael.graetzel@epfl.ch

[b] *Dr. B. E. Hardin,[+] Prof. M. D. McGehee*
Department of Materials Science and Engineering
Stanford University
California 94305 (USA)

[c] *E. T. Hoke*
Department of Applied Physics
Stanford University
California 94305 (USA)

[d] *Prof. T. Torres*
Departamento de Química Orgánica (C-I), Facultad de Ciencias
Universidad Autónoma de Madrid
Cantoblanco, 28049 Madrid, Spain

[e] *Prof. T. Torres*
IMDEA Nanoscience, Facultad de Ciencias, Cantoblanco, 28049 Madrid, Spain

[+] *These authors contributed equally to this work.*

Supporting information for this article is available on the WWW under http://dx.doi.org/10.1002/cphc.201000854.

Calculations suggest that a multi-step energy transfer process from the large-bandgap ERD (DCM) to the lower-bandgap ERD (RB) followed by FRET to the sensitizing dye is less significant in this system, but could be the dominant mechanism in some DSCs with multiple energy relay dyes.

2. Results and Discussion

2.1. Materials Properties and Förster Radius Calculations

DCM and RB were chosen as energy relay dyes because of their high absorption coefficients, excellent photoluminescence (PL) quantum efficiencies, and short PL lifetimes to minimize electrolytic quenching. DCM has a peak molar absorption coefficient, ε_{DCM}, of 44900 $M^{-1}cm^{-1}$ at 460 nm and a PL quantum efficiency of 44% in acetonitrile (Figure 1).[15–16] RB has a peak molar absorption coefficient of 106000 $M^{-1}cm^{-1}$ at 543 nm and a PL quantum efficiency of 70% in ethanol.[17] The

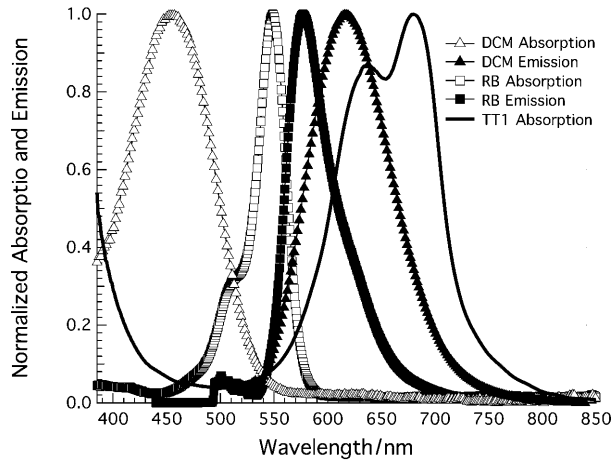

Figure 1. Absorption and emission spectra of DCM and RB energy relay dyes with TT1 as the sensitizing dye.

emission efficiency of RB in a 15/85 (v/v) mixture of valeronitrile and acetonitrile is 44.7%. The zinc phthalocyanine dye, TT1, was chosen as the sensitizing dye for its high molar absorption coefficient of 191500 $M^{-1}cm^{-1}$ at 680 nm.[10–11] High FRET rates are essential to quickly transfer the energy from the excited ERD before nonradiative decay. The FRET rate is related to the separation distance between donor and acceptor molecules and the Förster radius (R_0), the distance between two dye molecules where the energy transfer process has an efficiency of 50%. R_0 is dependent upon the ERD photoluminescence quantum efficiency (Φ_{PL}), the sensitizing dye peak absorption coefficient (ε) and the overlap between the emission of the ERD and the absorption of the sensitizing dye. The DCM and RB have good emission overlap with the absorption spectrum of the TT1 dye, as shown in Figure 1, resulting in Förster radii of 6.9 nm and 6.3 nm respectively (calculation shown in the Supporting Information). R_0 from DCM to RB is estimated to be 4 nm (Table 1).

Table 1. Photophysical properties of DCM and RB.

ERD	ε [$M^{-1}cm^{-1}$][a]	Φ_{PL} [%][b]	τ_0 [ns][c]	$R_{0,TT1}$ [nm][d]	$R_{0,RB}$ [nm][f]	PL_0/ PL[g]
DCM	44900	44.0	2.06	6.85	4.00	8.54
RB	106000	44.7	1.98	6.27	–	39.0

[a] Molar absorption coefficient of DCM in acetonitrile (at 460 nm) and RB in ethanol (at 543 nm). [b] Photoluminescence quantum efficiency in acetonitrile and valeronitrile. [c] Photoluminescence lifetime of 10^{-4} M ERD in acetonitrile and valeronitrile. [e] Förster radius from ERD to TT1. [f] Förster radius from DCM to RB. [g] Photoluminescence quenching: Both concentration and electrolyte quenching are taken into account.

2.2. Electrolyte and Concentration Quenching

Once excited, the ERD can transfer its energy to the sensitizing dye via FRET, emit a photon, or nonradiatively decay. The nonradiative decay rate of ERDs inside of a DSC can greatly increase due to concentration quenching of the ERD and by the presence of triiodide in the electrolyte.[18] The dynamic quenching of the ERD by the redox couple inside the electrolyte is relatively low according to our previous studies since DCM (τ_0 = 2.06 ns) and RB (τ_0 = 1.98 ns) have short photoluminescence lifetimes. Figure 2 shows that the fluorescence intensity is re-

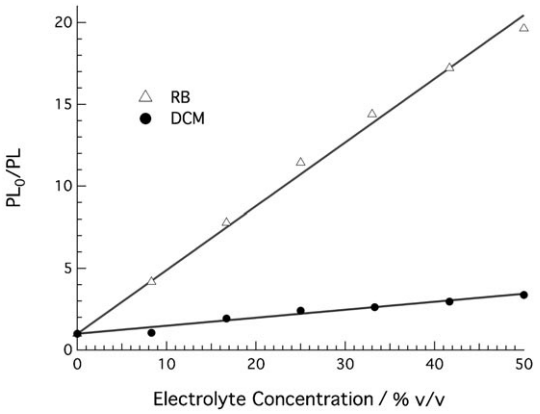

Figure 2. Influence of electrolyte concentration on PL Quenching of DCM and RB. Undiluted electrolyte composition: 0.6 M 1-butyl-3-methyl imidiazolium iodide, 0.025 M LiI, 0.04 M iodine, 0.05 M guanidinium thiocyanate, 0.28 M *tert*-butylpyridine in 15/85 (v/v) mixture of valeronitrile and acetonitrile.

duced with increasing concentration of the electrolyte. Although these dyes have similar PL lifetimes, quenching by the electrolyte enhances the nonradiative decay rate of DCM by 4.9 times and RB by 39 times. It is noted that the nonradiative decay rate can be determined by extrapolating the line to 100% of the electrolyte concentration. Concentration quenching can also play a significant role in nonradiative decay. DCM exists as both *cis* and *trans* photoisomers whose ratio is solvent- and concentration-dependent.[15] Increasing the DCM concentration from 10^{-4} M to 25 mM reduces the PL lifetime from 2 ns to 1.18 ns.[11] RB does not experience significant concentration quenching (< 10%) for the moderate concentrations (10–15 mM) used in DSCs. Combining the effects of both con-

centration quenching and electrolyte quenching increases the overall rate of PL quenching (PL_0/PL) of DCM by 8.54 times the normal decay rate.

2.3. Photovoltaic Performance

The photovoltaic performance parameters of the TT1-sensitized dye cells with and without the energy relay dyes are summarized in Table 2. Separately, DCM and RB augmented the short-circuit current density, J_{sc} by 26% and 16%, which dominantly contributed to increase the power conversion efficiency by 25% and 12%, respectively. Overall, the power conversion efficiency increased by 35% from incorporating the two relay dyes with complementary absorption spectra. Futhermore, the J_{sc} increased by 44%, which is the largest increase in J_{sc} due to energy relay dyes reported so far. Devices with both relay dyes exhibited an external quantum efficiency (EQE) of about 30% or higher over the entire visible spectrum (Figure 3) with a substantial improvement over the TT1 only control device in the 400–590 nm range due to light harvesting from the relay dyes.

Table 2. *J–V* characteristics of dye-sensitized solar cells with various ERDs.

Dye/ERD[a]	J_{sc} [mA cm^{-2}][b]	V_{oc} [mV][c]	*FF* [%][d]	η [%][e]
TT1	6.79	593	73	2.94
TT1/DCM	8.53 (26%)	599 (1.0%)	72 (−1.4%)	3.68 (25%)
TT1/RB	7.88 (16%)	580 (−2.2%)	72 (−1.4%)	3.29 (12%)
TT1/DCM/RB	9.81 (45%)	579 (−2.4%)	70 (−4.3%)	3.97 (35%)

[a] [DCM] = 22 mM and [RB] = 20 mM in the electrolyte. [b] The short-circuit current density at 100 mW cm^{-2}. [c] The open-circuit voltage. [d] The fill factor. [e] The power conversion efficiency derived from $J_{sc}V_{oc}FF/I_0$ (100 mW cm^{-2}). Values in parenthesis are changes of *J–V* characteristics compared to TT1-based solar cell.

The presence of the relay dyes decreased the EQE slightly in the 600–710 nm range where the sensitizing dye strongly absorbs. This decrease is likely due to the ability of the RB dye with its carboxylic acid binding group to displace some TT1 dye molecules on the TiO_2 surface or a RB-TT1 charge transfer. We also considered the possibility that absorption by RB might decrease the amount of light available for the TT1 dye to absorb; however, the largest decrease in the EQE is at 700 nm where this effect should be negligible.

We investigated the possibility that the increase in performance from adding RB could be due to RB attaching to the TiO_2 surface and directly injecting charge when excited. The RB dye was replaced with an ester of the dye (RB E, Scheme 1) to prevent dye attachment to titania. RB E containing devices showed an increase in the EQE over the control TT1 devices in the 470–590 nm range which is only 8% lower than the TT1/RB devices (Supporting Information, Figure S1). This suggests that the added photoresponse from the RB dye between 470–590 nm is primarily due to FRET from RB to TT1 (92%) while direct injection plays a relatively small role (8%).

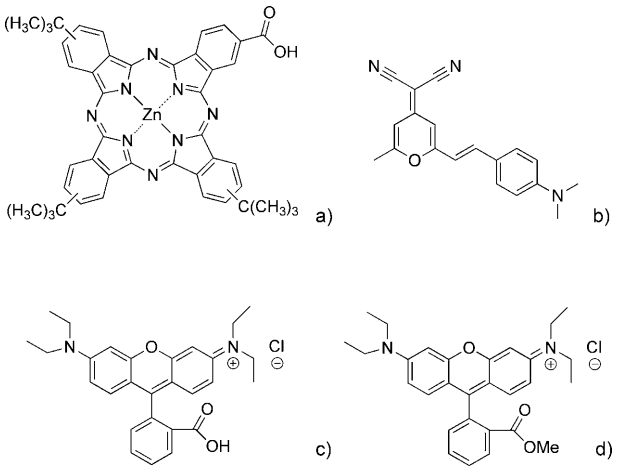

Scheme 1. Molecular structures of a) TT1, b) DCM, c) RB, and d) RB E.

The excitation transfer efficiency ($\overline{ETE}$) is the probability that an excited ERD (i.e. DCM or RB) transfers its energy to the sensitizing dye (i.e. TT1).[4] The $\overline{ETE}$ for the DCM dye to TT1 was previously shown to be greater than 95%.[11] The $\overline{ETE}$ of RB was estimated to be 34% using the maximum measured increase in EQE due to RB E (19%) in the TT1/RB E devices (see supplemental Figure S2). The calculated fraction of light absorbed by RB at this wavelength was 79%. The internal quantum efficiency (IQE) was estimated to be 80% based on the peak EQE at 680 nm (70%) and the calculated absorption by the TT1 dye at this wavelength (87.5%). The lower $\overline{ETE}$ value of RB is ascribed to the higher quenching compared to DCM.

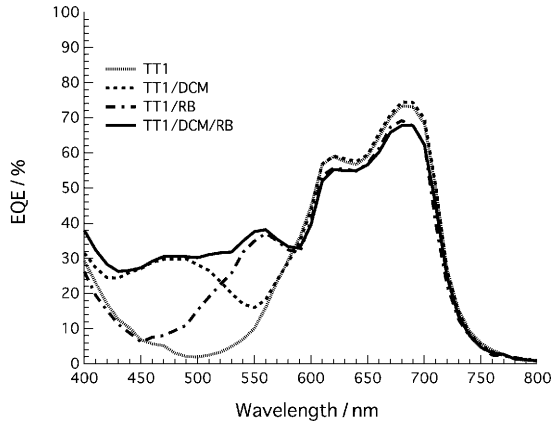

Figure 3. The EQEs of dye-sensitized solar cells with various ERDs.

2.4. Calculating Energy Transfer Efficiencies from DCM to RB or TT1

Theoretical calculations for the $\overline{ETE}$ have been performed for donors and acceptors in a variety of geometries and distributions[19–21] and E. T. Hoke et al. have recently shown a comprehensive model to compute the quantitative $\overline{ETE}$ in DSCs.[22] Once excited, DCM can undergo energy transfer to both the

RB relay dye and the TT1 sensitizing dye. Energy transfer efficiency calculations were performed to determine whether there is appreciable energy transfer occurring from DCM to RB which would compete with direct energy transfer to TT1 that could influence the $\overline{ETE}$ of the DCM. In our model, the mesopores were approximated as cylinders or spheres with a pore diameter of 20 nm, which is roughly the mean pore size in the DSC devices as determined from BET measurements.[11] The DCM and RB ERDs were assumed to be randomly distributed in the mesopores, while the TT1 sensitizing dye densely covered the pore walls. Additional details about the model can be found in the Supporting Information.

Energy transfer from DCM to TT1 was found to be the dominant process occurring after the DCM is excited for both pore geometries (Table 3). Energy transfer from DCM to RB occurs with only an 11% probability in spherical pores and 18% in the cylindrical pores. Thus the dominant light-harvesting pathway for photoexcited DCM dyes is through energy transfer to TT1, while the multistep FRET to RB followed by FRET to TT1 is relatively minor.

Table 3. Average FRET yields from DCM over the pore volume for 20 nm diameter pores.

Pore Geometry	No FRET [%]	FRET to TT1 [%]	FRET to RB [%]
Sphere	1.0	87.7	11.3
Cylinder	2.3	79.3	18.4

The two-step FRET mechanism can be beneficial or detrimental to the overall $\overline{ETE}$ of the large-bandgap relay dye (i.e. DCM) depending upon how efficiently the two relay dyes can transfer their energy to the sensitizing dye. It is somewhat surprising that adding RB to the TT1/DCM devices does not decrease light harvesting by the DCM (below 500 nm, see Figure 3) via the two-step FRET mechanism given that RB is significantly less efficient at transferring energy to TT1 ($\overline{ETE}$ = 34%) than DCM ($\overline{ETE}$ > 95%). This, however, can be explained by examining the decay probabilities of DCM molecules located at different distances from the pore center (see Figure 4 for the TT1/DCM/RB device and the Supporting Information, Figure S2 for the TT1/DCM device). In the TT1/DCM device, the DCM excitations that decay by electrolytic quenching of fluorescence before FRET can occur are lost primarily in the center of the pore where FRET to TT1 is least efficient. In the TT1/DCM/RB device, an excited DCM molecule in the center of the pore has the additional possibility of undergoing FRET to a random nearby RB molecule, which will most likely be closer to the pore wall. This is beneficial to light harvesting, since FRET becomes substantially more efficient if the excited relay dye is closer to the sensitizing dye. Energy transfer to RB is also more likely to occur for DCM dyes in the center of the pore where it can be beneficial, while it is negligible near the pore wall where transfer to a random RB molecule would on average detrimentally move the excitation away from the pore wall.

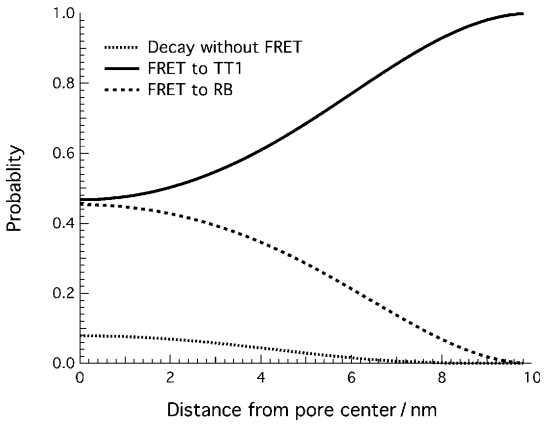

Figure 4. Decay probability from DCM as a function of DCM's distance from the pore center in a spherical pore 20 nm in diameter.

3. Conclusions

We demonstrated that multiple relay dyes can extend the panchromatic response of dye-sensitized solar cells and improve photovoltaic performance by 35%. Both ERDs show a new photoresponse, adding over 30% IPCE from 400–590 nm. This work demonstrates that FRET processes from multiple energy relay dyes to a sensitizing dye can be efficient enough for ERDs to be incorporated into state-of-the-art DSC systems. FRET from both relay dyes to the sensitizing dye was calculated to be the dominant mechanism for increased light harvesting. Energy transfer from one relay dye to the other is less important in this system but could play an important role in other DSC with multiple relay dyes. The device performance for this dye system was ultimately limited by quenching of RB by the electrolyte and the solubility of DCM.[11] Future relay dye systems should be developed with highly soluble dyes with short fluorescence lifetimes which are more inert to quenching by the iodide/triiodide or alternative redox couples. This will enable increased light absorption from larger dye loading and minimize the impact of electrolytic and concentration quenching, providing a pathway toward higher efficiency devices.

Experimental Section

Materials: Rhodamine B methyl ester has been prepared following a slightly modified literature procedure.[23] Acetyl chloride (3 mL) was added drop-wise to a stirred mixture of rhodamine B (**1**, 500 mg, 1.04 mmol) and methanol (100 mL). The reaction mixture was heated at 50 °C under an atmosphere of argon and 2 mL of acetyl chloride were added every 24 h. After 3 days the reaction was not evolving anymore as checked by TLC. After cooling down to room temperature the volatiles were evaporated under vacuum. This crude contains about 10% of the acid rhodamine B. Purification was achieved by silica gel chromatography column eluting with acetone/methanol 1%. Once all front impurities are removed, the product is eluted with acetone/methanol 2%/water 1%. The ester was obtained as a hygroscopic amorphous solid (213 mg, yield 41%).

^{1}H NMR (400 MHz, D_6-DMSO): $\delta = 8.24$ (1H, dd, $J = 7.6$, 1.2 Hz); 7.90 (1H, dt, $J = 7.2$, 1.6 Hz); 7.82 (1H, dt, $J = 7.2$, 1.2 Hz); 7.48 (1H, dd, $J = 6.4$, 1.2 Hz); 7.05 (2H, dd, $J = 9.6$, 2.4 Hz); 6.98–6.94 (4H, m), 3.61 (8H, q, $J = 7.2$ Hz); 3.57 (3H, s); 1.18 ppm (12H, t, $J = 7.2$ Hz).

Characterization Techniques: Time-resolved PL measurements were performed using a time-correlated single-photon-counting (TCSPC) system from PicoQuant. Solutions were excited with a pulsed laser diode, (model LDH 485: 481 nm, 70 ps FWHM, 5 MHz) detected with a single photon avalanche diode (PDM 100CT SPAD) attached to a monochromator and processed by a PicoHarp 300 correlating system.

For photovoltaic measurements of the DSCs, the irradiation source was a 450 W xenon light source (Osram XBO 450, Germany) with a filter (Schott 113), whose power was regulated to the AM 1.5G solar standard by using a reference Si photodiode equipped with a colour-matched filter (KG-3, Schott) in order to reduce the mismatch in the region of 350–750 nm between the simulated light and AM 1.5G to less than 4%. The measurement of incident photon-to-current conversion efficiency (IPCE) was plotted as a function of excitation wavelength by using the incident light from a 300 W xenon lamp (ILC Technology, USA), which was focused through a Gemini-180 double monochromator (Jobin Yvon Ltd.). The measurement settling time between applying a voltage and measuring a current for the I–V characterization of DSSCs was fixed to 40 ms.

DSC Fabrication: Details can be found elsewhere.[11] Briefly, FTO glass plates (Nippon Sheet Glass, Solar 4 mm thickness) were used for supporting TiO_2 layer after a $TiCl_4$ treatment. A paste composed of 17 nm anatase TiO_2 particles for the transparent nanocrystalline layer was coated on the FTO glass plates by screen printing. The thickness reached to a required one after a repeated coating-drying procedure. The TiO_2 electrodes were made of ~5.4 μm transparent layer composed of 17 nm sized anatase. The TiO_2 electrodes were gradually heated under air flow. After a second $TiCl_4$ treatment, the TiO_2 electrodes were immersed into a 0.1 mM solution of TT1 with 10 mM of chenodeoxycholic acid in ethanol and kept at room temperature for 5 h. The large concentration of chenodeoxycholic acid is needed to co-absorb to the TiO_2 surface to reduce TT1 aggregation.[24] The applied electrolyte was composed of 0.6 M 1-butyl-3-methyl imidiazolium iodide (BMII), 0.025 M LiI, 0.04 M iodine, 0.05 M guanidinium thiocyanate, 0.28 M *tert*-butylpyridine in 15/85 (v/v) mixture of valeronitrile and acetonitrile. In order to study the effect of multiple ERDs, 22 mM DCM and 20 mM RB were added in the above electrolyte. The dye-adsorbed TiO_2 electrode and counter electrode were assembled into a sealed sandwich-type cell with a gap of a hot-melt ionomer film, Surlyn (25 μm, Du Pont). In order to reduce scattered light from the edge of the glass electrodes of the dyed TiO_2 layer, a light-shading mask was used onto the DSCs, so the active area of DSCs was fixed to 0.2 cm^2.

Acknowledgements

The EPFL-affiliated authors thank the Swiss National Science Foundation for Financial Support. E. T. Hoke was funded by the Fannie and John Hertz Foundation. M. Grätzel and T. Torres were supported by EU Project ROBUST DSC, FP7-Energy-2007–1-RTD. This publication is partially based on work supported by the Center for Advanced Molecular Photovoltaics (Award No KUS-C1–015–21), made by King Abdullah University of Science and Technology (KAUST) gratefully acknowledged by M. Grätzel and M. McGehee. Financial support by the MEC, Spain (CTQ2008–00418/BQU, CONSOLIDER-INGENIO 2010 CDS 2007–00010, PLE2009–0070), and CAM (MADRISOLAR-2, S2009/PPQ/1533), is gratefully acknowledged by T. Torres.

Keywords: dyes/pigments · dye-sensitized solar cells · FRET · photochemistry · photovoltaics

[1] M. Grätzel, *Acc. Chem. Res.* **2009**, *42*, 1788.
[2] J.-H. Yum, E. Baranoff, S. Wenger, M. K. Nazeeruddin, M. Grätzel, *Energy Environ. Sci.*, DOI: 10.1039/C0EE00536C.
[3] C. Siegers, J. Hohl-Ebinger, B. Zimmerrnann, U. Wurfel, R. Mulhaupt, A. Hinsch, R. Haag, *ChemPhysChem* **2007**, *8*, 1548.
[4] B. E. Hardin, E. T. Hoke, P. B. Armstrong, J.-H. Yum, T. Torres, J. M. J. Fréchet, M. K. Nazeeruddin, M. Grätzel, M. D. Mcgehee, *Nat. Photonics* **2009**, *3*, 406.
[5] J.-H. Yum, B. E. Hardin, S.-J. Moon, E. Baranoff, F. Nuesch, M. D. McGehee, M. Grätzel, M. K. Nazeeruddin, *Angew. Chem.* **2009**, *121*, 9441; *Angew. Chem. Int. Ed.* **2009**, *48*, 9277.
[6] G. K. Mor, J. Basham, M. Paulose, S. Kim, O. K. Varghese, A. Vaish, S. Yoriya, C. A. Grimes, *Nano Lett.* **2010**, *10*, 2387.
[7] J.-H. Yum, E. Baranoff, B. E. Hardin, E. T. Hoke, M. D. McGehee, F. Nüesch, M. Grätzel, M. K. Nazeeruddin, *Energy Environ. Sci.* **2010**, *3*, 434.
[8] T. Förster, *Ann. Phys.* **1948**, *437*, 55.
[9] P. R. Hammond, *Opt. Commun.* **1979**, *29*, 331.
[10] J.-J. Cid, J.-H. Yum, S.-R. Jang, M. K. Nazeeruddin, E. Martinez-Ferrero, E. Palomares, J. Ko, M. Grätzel, T. Torres, *Angew. Chem.* **2007**, *119*, 8510; *Angew. Chem. Int. Ed.* **2007**, *46*, 8358.
[11] B. E. Hardin, J.-H. Yum, E. T. Hoke, Y. C. Jun, P. Péchy, T. Torres, M. L. Brongersma, M. K. Nazeeruddin, M. Grätzel, M. D. McGehee, *Nano Lett.* **2010**, *10*, 3077.
[12] A. Ehret, L. Stuhl, M. T. Spitler, *J. Phys. Chem. B* **2001**, *105*, 9960.
[13] J.-H. Yum, S. R. Jang, P. Walter, T. Geiger, F. Nuesch, S. Kim, J. Ko, M. Grätzel, M. K. Nazeeruddin, *Chem. Commun.* **2007**, 4680.
[14] T. Karstens, K. Kobs, *J. Phys. Chem.* **1980**, *84*, 1871.
[15] J. M. Drake, M. L. Lesiecki, D. M. Camaioni, *Chem. Phys. Lett.* **1985**, *113*, 530.
[16] J. Bourson, B. Valeur, *J. Phys. Chem.* **1989**, *93*, 3871.
[17] F. L. Arbeloa, P. R. Ojeda, I. L. Arbeloa, *J. Lumin.* **1989**, *44*, 105.
[18] J. R. Lakowicz, *Principles of Fluorescence Spectroscopy, 2nd Ed.*, Plenum Press, New York, **1999**.
[19] B. K. K. Fung, L. Stryer, *Biochemistry* **1978**, *17*, 5241.
[20] J. Klafter, A. Blumen, *J. Lumin.* **1985**, *34*, 77.
[21] A. Blumen, J. Klafter, G. Zumofen, *J. Chem. Phys.* **1986**, *84*, 1397.
[22] E. T. Hoke, B. E. Hardin, M. D. McGehee, *Opt. Express* **2010**, *18*, 3893.
[23] J. A. Ross, B. P. Ross, K. L. Cosgrove, H. Rubinsztein-Dunlop, R. P. McGeary, *Molbank* **2006**, M515.
[24] J.-H. Yum, S.-R. Jang, R. Humphry-Baker, M. Grätzel, J.-J. Cid, T. Torres, M. K. Nazeeruddin, *Langmuir* **2008**, *24*, 5636.

Received: October 11, 2010
Revised: November 30, 2010
Published online on January 5, 2011

